Advanced Computational Electromagnetics
T. Honma (Ed.)
IOS Press, 1995

CURRENT CONDUCTING PATH ESTIMATION FROM THE LOCALLY MEASURED MAGNETIC AND ELECTRIC FIELDS

Tatsuya DOI, Seiji HAYANO, and Yoshifuru SAITO

College of Engineering, Hosei University,
3-7-2 Kajino, Koganei, Tokyo 184, JAPAN

Nondestructive testing of the electric power appratus is one of the most important problems in order to maintain the high reliability. For example, electric power supplies used for the large scale computers are sealed to a box with coolant. This means that the current conducting path in the box should be estimated from the electromagnetic fields measured on the surface enclosing the box. This paper proposes one of the novel approaches for the current conducting path estimation from the locally measured magnetic and electric fields. Key idea of our method is a generalization of the method of vector arrow map proposed for the human heart diagnosis.

1. INTRODUCTION

With the developments of modern SQUID flux meter, the magnetocardiography (MCG) and magnetoencephalography (MEG) are intensively studied for the medical applications of human heart's and of human brain's functional operation, respectively. Particularly, the signals of MCG are relatively large compared with those of MEG so that MCG may be considered as one of the most effective methodologies for the human heart diagnosis. A method of MCG diagnosis is to plot the current density vector arrow map obtained by taking the rotation of measured magnetic field normal to the body surface above human heart. According to the previous investigations, it has been clarified that the method of current density vector arrow map is quite effective to the human heart diagnosis [1]. On the other side, electrocardiography (ECG) is currently used as a quite popular and standard method for human heart diagnosis [2].

In the present paper, we generalize the method of vector arrow map proposed for the human heart diagnosis to the electric field vector arrow map in order to obtain the power density distribution on a surface of some target containing current conducting path. FEM simulation shows that the power density distribution on a surface corresponds to an image of current conducting path projected onto the surface. Thus, it is revealed when we can measure the electric potentials and magnetic fields on the

surface enclosing target, it is possible to estimate the global current conducting path in the target.

2. CURRENT CONDUCTING PATH ESTIMATION

2.1. Electrical conduction system in human heart

The electrical activity initiating the heartbeat takes place at sino-atrial node. This region of the heart is located at the endocardial surface of the right atrium at the junction of the superior vena cava. The tissue in this region, about the diameter of pencil lead and 2.4cm in length, is highly specialized. These cells do not remain at rest but slowly depolarized until threshold is reached whereupon (self) excitation takes place. Such cells, known as pacemakers, are responsible for initiation of the heartbeat through excitation of their neighbors. The concatenation of activity works contiguously until all tissue has been excited. Atrial activity is conducted to the ventricles only through specialized tissue constituting the atrioventricular (AV) junction. This tissue is characterized by its very slow propagation velocity. Once the impulse reaches the ventricular exit, it propagates at an elevated velocity through the conduction bundles of His and a network of Purkinje fibers which convey the impulse to many endocardial sites in the left and right ventricles and the septum. Functionally, the AV delay serves to separate in time atrial from ventricular contraction. The conduction tissue is characterized by its relative high velocity of 2m/s, in contrast with the 0.5m/s of ventricular muscle; it is specialized for conduction and contains little contractile elements. The consequence of excitation of many endocardial sites at nearly the same time is broad depolarization waves throughout the ventricles leading to a uniform and sequenced muscular contraction.

2.2. Modeling of conducting system and FEM simulation

As described above, the conducting system of human heart may be regarded as one of the materials having larger conductivity compared with the other parts so that we consider a rectangular prism which is composed of the two materials. One has a large conductivity and the other has a small conductivity. Further, frequency of the electrical pulse exciting the movement of heart muscle is relatively low, i.e. about 1Hz, therefore, the system is assumed to an electrostatic system governed by a following Laplace equation:

$$\nabla \cdot (\kappa \nabla \phi) = 0, \tag{1}$$

where κ and ϕ denote the conductivity and electric potential, respectively.

Equation (1) is discretized by the finite element method for the target rectangular prism. Imposing the boundary conditions, i.e. one of the discretized points is set to a unit voltage and the other one discretized point is set to zero voltage, we have a

following system equation:

$$\mathbf{CX} = \mathbf{Y}, \tag{2}$$

where C, **X** and **Y** are the system matrix, potential vector and input vector determined by the Dirchlet type boundary condition, respectively.

After solving (2), a current density **J** distribution in a rectangular prism is obtained by means of the following Ohm's law:

$$\mathbf{J} = -\kappa(\nabla\phi). \tag{3}$$

Figure 1(a) shows an example of current density distribution in a rectangular prism. The accompanying electric potentials on the top surface of this rectangular prism

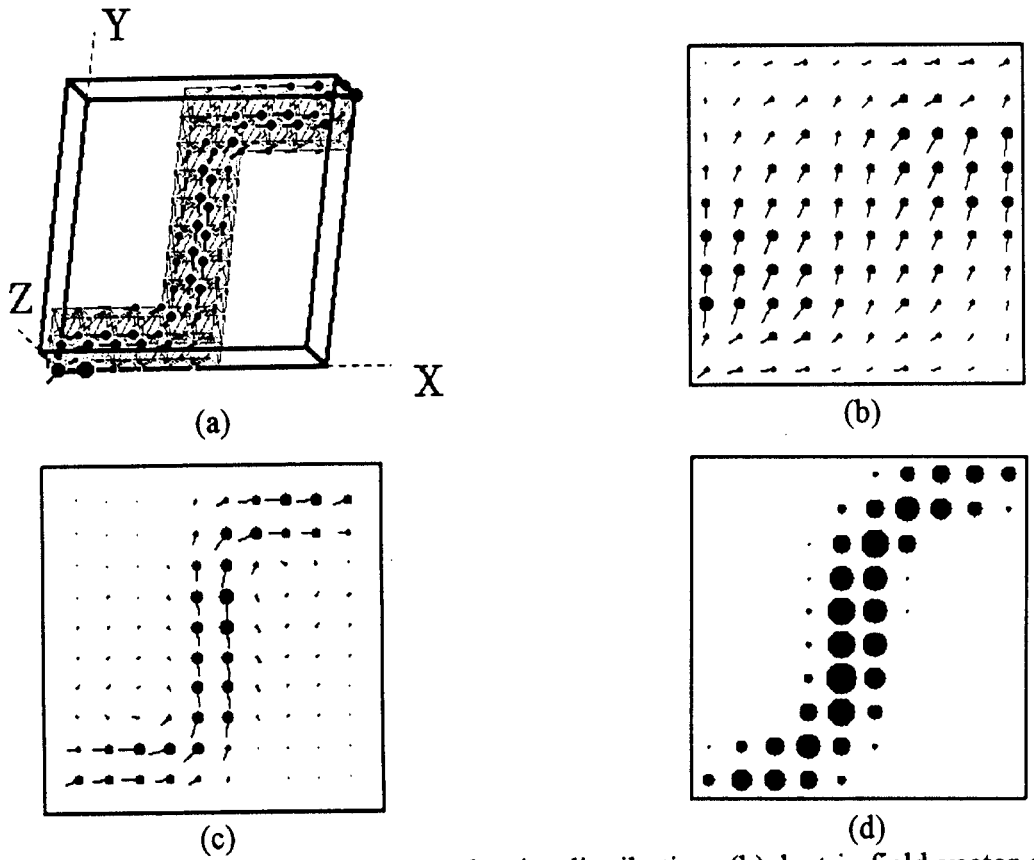

Fig. 1. Simulated results. (a)Current density distribution, (b)electric field vector arrow map, (c)current density vector arrow map, and (d)power density distribution on the top surface of the thin rectangular prism. The high current density parts correspond to the conducting path and this conducting path is projected onto the top surface as the high power density distributed part in (d).

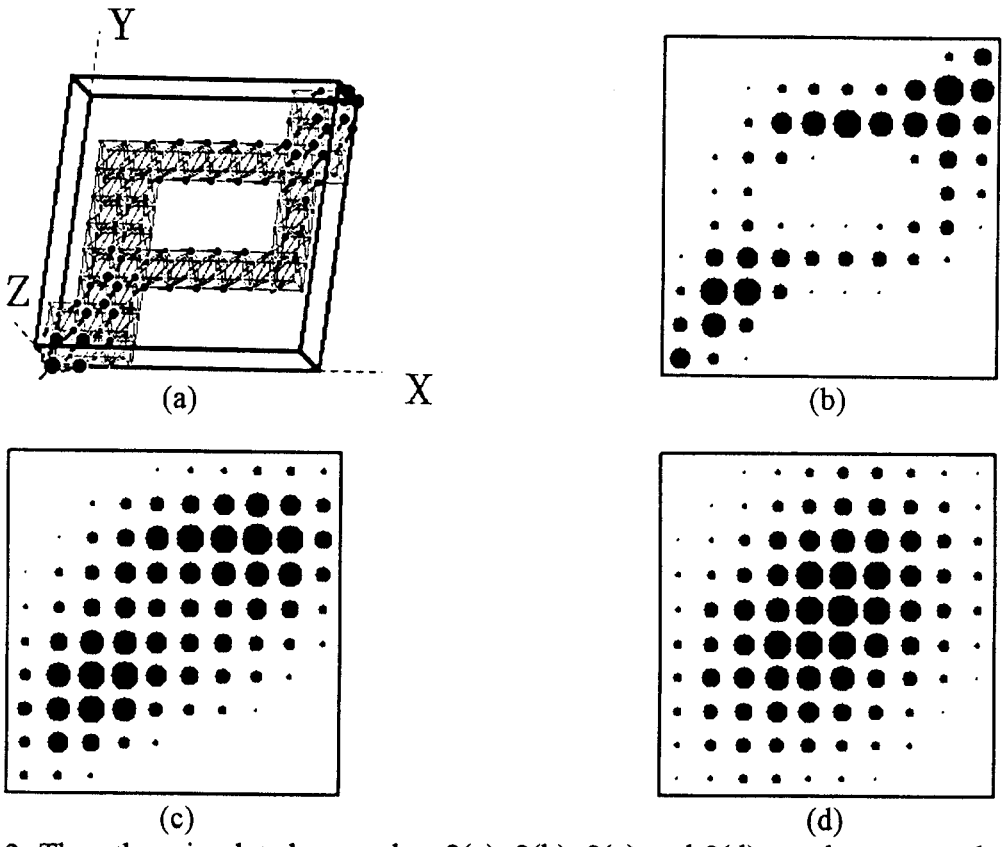

Fig. 2. The other simulated examples. 2(a), 2(b), 2(c) and 2(d) are the current density distribution, power density distribution on the top surface of a thin rectangular prism, power density distribution on the top surface of a rectangular prism having three times thickness of 2(b), and power density distribution on the top surface of a rectangular prism having seven times thickness of 2(b), respectively.

corresponds to an ECG. Taking a gradient of the potential yields an electric field vector arrow map shown in Fig. 1(b). The current density J in (3) causes the static magnetic fields normal to the top surface, and this magnetic field distribution corresponds to a MCG. Taking a rotation of the magnetic field yields a current density vector arrow map shown in Fig. 1(c). Finally, taking an inner product between the electric field and current density at each position yields a power density distribution on the top surface. Figure 1(d) shows a power density distribution on the top surface. Comparison Figs. 1(a) and 1(d) suggests that the current path is projected on the top surface. Thus, the conducting path can be identified by means of our approach with higher accuracy when the conducting path is located in parallel to the top surface.

Figure 2 shows the other simulated examples. Figures 2(a), 2(b), 2(c) and 2(d) are the current density distribution, surface power density distribution on the top of a thin rectangular prism, power density distribution on the top surface a rectangular prism having three times thickness of 2(b), and power density distribution on the top surface of a rectangular prism having seven times thickness of 2(b), respectively.

The results in Fig. 2 suggest that the power density distribution corresponds well to the conducting path only if the conducting path is located near to the top surface. However, it is possible to identify a global conducting path even if the target conducting path is somewhat far from the measurement surface.

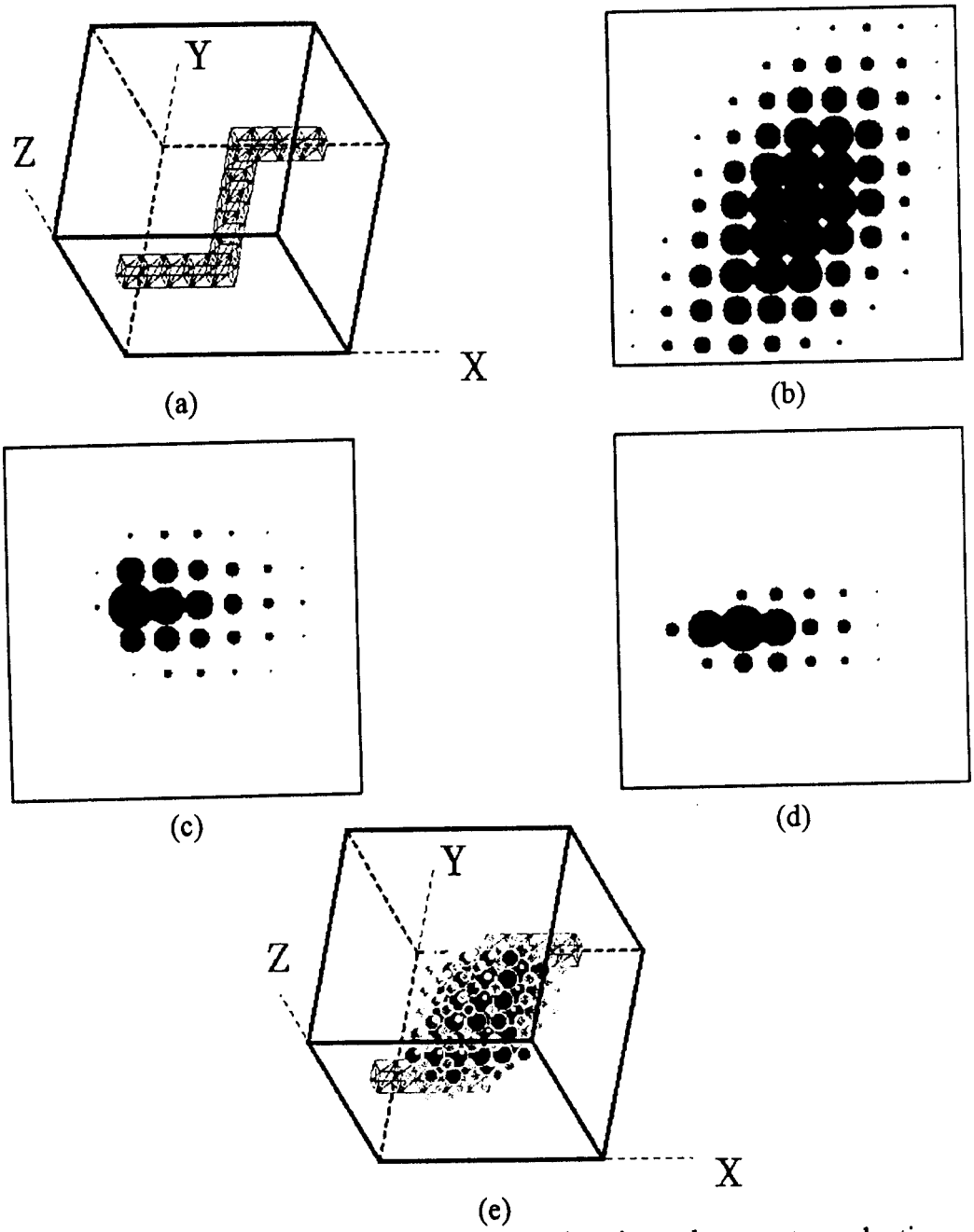

Fig. 3. Surface power density distributions and estimated current conducting path. (a)Exact current conducting path, (b)top surface power distribution, (c)left surface power density distribution, (d)front surface power density distribution, and (e)estimated current conducting path.

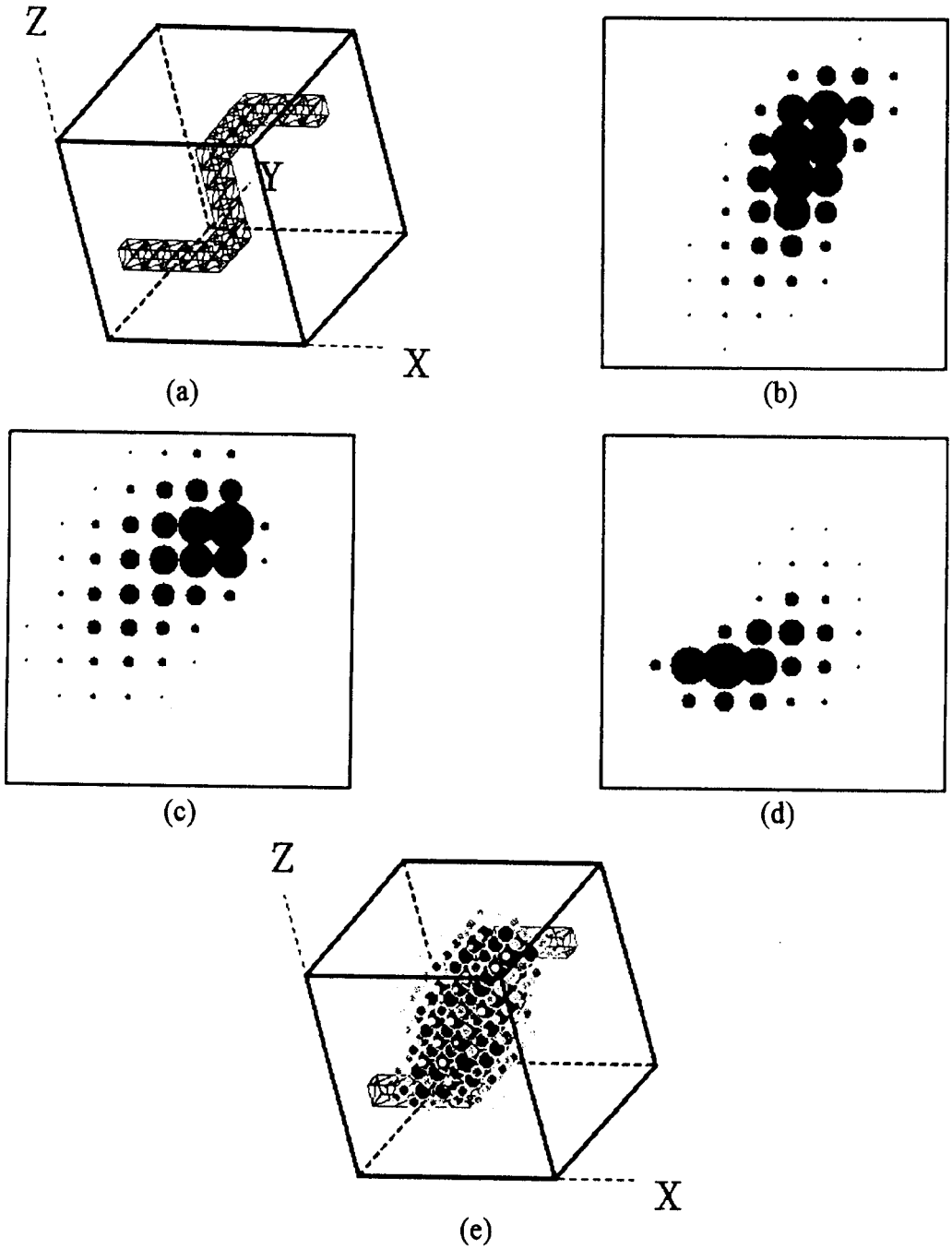

Fig. 4. Surface power density distributions and estimated current conducting path. (a)Exact current conducting path, (b)top surface power density distribution, (c)right surface power density distribution, (d)front surface power density distribution, and (e)estimated current conducting path.

2.3. Application to the current conducting path estimation

Figures 3 and 4 show examples of the application to the current conducting path estimation.

Figure 3(a) shows an exact current conducting path in a rectangular box. Figures 3(b), 3(c) and 3(d) show the power density distributions on the top, left and front surfaces, respectively.

The power density distributions of the other surfaces can be obtained in a similar manner. Using the entire surfaces power density distributions, the current conducting path can be estimated by projecting them to the interior of box. Figure 3(e) shows the estimated current conducting path. Similar to those of figure 3, figure 4 shows the other example. Thus, we have succeeded in estimating the current conducting path from the locally measured electric and magnetic fields.

3. CONCLUSION

In the present paper, we have generalized the method of vector arrow map proposed for the human heart diagnosis to the electric field vector arrow map in order to obtain the power density distribution on a surface of some target containing current conducting path. FEM simulation has shown that the power density distribution on a surface corresponds to an image of current conducting path projected onto the surface. Thus, it has been revealed when we can measure the electric potentials and magnetic fields on the surface enclosing target, it is possible to estimate the global current conducting path in the target.

REFERENCES

[1] K.Watanabe et al., Biomagnetism'87 Eds. K.Atsumi et al. (Tokyo Denki University Press, Japan 1988)pp.346-349.

[2] Y.Nakaya et al., Journal of Electrocardiography 21 (2),(1988)pp.168-173.